Journal of Biomechanics xxx (2018) xxx–xxx

Contents lists available at ScienceDirect

Journal of Biomechanics

journal homepage: www.elsevier.com/locate/jbiomech
www.JBiomech.com

Short communication

Experimental evaluation of current and novel approximations of articular surfaces of the ankle joint

Claudio Belvedere [a,*], Sorin Siegler [b], Andrea Ensini [c], Jason Toy [b], Paolo Caravaggi [a], Ramya Namani [b], Luca Giuseppe Princi [a], Stefano Durante [d], Alberto Leardini [a]

[a] Movement Analysis Laboratory, IRCCS Istituto Ortopedico Rizzoli, Bologna, Italy
[b] Department of Mechanical Engineering and Mechanics, Drexel University, Philadelphia, PA, USA
[c] 1st Orthopedic-Traumatologic Clinic, IRCCS Istituto Ortopedico Rizzoli, Bologna, Italy
[d] Nursing, Technical and Rehabilitation Assistance Service, IRCCS Istituto Ortopedico Rizzoli, Bologna, Italy

ARTICLE INFO

Article history:
Accepted 14 April 2018
Available online xxxx

Keywords:
Ankle
Replacement
Morphology
Articular surfaces
Kinematics
Flexibility
In-vitro

ABSTRACT

Kinematics and flexibility properties of both natural and replaced ankle joints are affected by the geometry of the articulating surfaces. Recent studies proposed an original saddle-shaped, skewed, truncated cone with laterally oriented apex, as tibiotalar contact surfaces for ankle prosthesis. The goal of this study was to compare *in vitro* this novel design with traditional cylindrical or medially centered conic geometries in terms of their ability to replicate the natural ankle joint mechanics. Ten lower limb cadaver specimens underwent a validated process of custom design for the replacement of the natural ankle joint. The process included medical imaging, 3D modeling and printing of implantable sets of artificial articular surfaces based on these three geometries. Kinematics and flexibility of the overall ankle complex, along with the separate ankle and subtalar joints, were measured under cyclic loading. In the neutral and in maximum plantarflexion positions, the range of motion under torques in the three anatomical planes of the three custom artificial surfaces was not significantly different from that of the natural surfaces. In maximum dorsiflexion the difference was significant for all three artificial surfaces at the ankle complex, and only for the cylindrical and medially centered conic geometries at the tibiotalar joint. Natural joint flexibility was restored by the artificial surfaces nearly in all positions. The present study provides experimental support for designing articular surfaces matching the specific morphology of the ankle to be replace, and lays the foundations of the overall process for designing and manufacturing patient-specific total ankle replacements.

1. Introduction

Total ankle replacement (TAR) is frequently performed for the treatment of end-stage ankle osteoarthritis. Unlike total hip and knee joint replacements, this treatment still suffers from high failure rates and clinical complications, in addition to low patient's satisfaction (Bartel and Roukis, 2015; Spirt et al., 2004). The ability to reproduce the original natural mobility and stability of the ankle joint complex with TAR has been recognized as a key factor for the clinical success of this surgical treatment (Giannini et al., 2010; Leardini et al., 2004). In more mechanical terms, the goal of TAR is to replicate the original range and pattern of rotations, hereinafter referred to as kinematics, and also the original rotational response to external torques, hereinafter referred to as flexibility (or laxity as in Belvedere et al., 2017). Because morphology and function at the ankle joint are complex (Leardini et al., 1999; Lundberg et al., 1989; Siegler et al., 1988), a major TAR design challenge is to produce artificial articular surfaces that best approximate morphology to possibly restore function, as observed in the intact ankle. Original studies on functional morphology of the ankle (Close, 1956; Hicks, 1953; Barnett and Napier, 1952; Close and Inman, 1952) established a single fixed axis of rotation at the tibiotalar joint, and a cylindrical or conical approximation for the talar dome, the latter having the apex on the medial side of the joint (Inman, 1976; Close and Inman, 1952). A recent image-based 3D study showed that the trochlear surface of the talus, and the articulating distal tibial surface, can be approximated by a saddle-shaped skewed truncated cone with laterally oriented apex (SSCL) (Siegler et al., 2014). This was recently supported by experimental evidence *in vitro* (Belvedere et al., 2017). Different

* Corresponding author at: Movement Analysis Laboratory, IRCCS Istituto Ortopedico Rizzoli, Via di Barbiano 1/10, Bologna, Italy.
E-mail address: belvedere@ior.it (C. Belvedere).

https://doi.org/10.1016/j.jbiomech.2018.04.024
0021-9290/© 2018 Elsevier Ltd. All rights reserved.

geometrical approximations of the artificial articular surfaces of TAR designs would result in different kinematics and flexibility at the replaced ankle, and, in the long term, in different clinical outcomes.

A previous paper from the present authors (Belvedere et al., 2017) has established the reliability of an experimental *in vitro* procedure to assess TAR implants, and the performance of the SSCL surfaces. The goal of the present study was to use this technique to compare the effect, in terms of kinematics and flexibility at the replaced ankle, of three possible different articular surfaces: the SSCL, a cylindrical, and a conical with apex oriented medially. The latter two are used in the large majority of the current TAR designs. For this purpose, custom 3D-printed implants, based on the three concepts mentioned above, were originally produced from 3D computer models of articulating bones.

2. Materials and methods

The overall procedures for implants design and manufacturing, experimental set-up and protocol, specimens population, and most of the data analysis have been previously reported (Belvedere et al., 2017). Briefly, ten cadaver legs disarticulated at the knee were defrosted at room temperature, and relevant radiographic images and surgeon inspections excluded ankle deformities or instability and cartilage defects. For each specimen, computer-tomography scans were processed (Analyze Direct™, Overland Park, KS-USA) to obtain 3D models of the tibia, fibula, talus and calcaneus. These were further processed (Geomagic™, Morrisville, NC-USA) to extract specimen-specific design parameters required to produce three different artificial surface approximations of the natural joint surfaces, as follow (Fig. 1): SSCL, matching saddle-shaped truncated cones with laterally oriented apex resulting from subject-specific anatomy (Belvedere et al., 2017; Siegler et al., 2014); cylindrical (CYL), matching cylindrical surfaces with the talar dome radius being the average between the radii of the relevant medial and lateral crest contours; and truncated-cone with a fixed medially-oriented apex (TCM) as claimed by Inman (1976). The final design of these three implants, consisting each of a tibial and a talar component, was performed using Inventor™ (AutoDesk, San Rafael, CA-USA). CYL and TCM are meant to represent the articulating geometry of most current TAR designs (Kakkar and Siddique, 2011; Lewis, 1994). The components were fixed to the bone via screws in their frontal aspect. At the distal tibia, two parallel tunnels drilled from the front were used as references to register bone models and the implants. The three implants were 3D-printed (Dimensions Elite™ by Stratasys, Inc.; nominal spatial resolution 0.2 mm) in acrylonitrile-butadienestyrene.

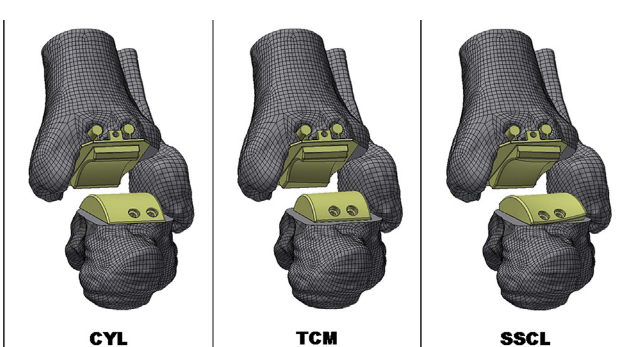

Fig. 1. Model rendering from the analysis of one typical specimen, after the design of the three implant sets: cylindrical-CYL (left), truncated-cone with medial apex – TCM (centre), and saddle shaped skewed truncated cone with laterally oriented apex – SSCL (right). The replaced joint is separated just to illustrate better the artificial surfaces.

Following surgical preparation of the specimen (Belvedere et al., 2017), each implant set was inserted, one at a time, and secured to the corresponding bone. Before and after each implantation, tests were performed to determine their corresponding mechanical response under these four conditions: with the natural surfaces (NATURAL), and following the replacement of the natural surfaces with the CYL, TCM, and SSCL implants. For this purpose, an Ankle Flexibility Tester (AFT, (Belvedere et al., 2017; Siegler et al., 1996)), and an optoelectronic stereo-photogrammetric system (Stryker Knee Navigation System, Stryker®, Kalamazoo, MI-USA (Belvedere et al., 2014)) were used. This whole experimental setup was able to apply and measure continuous torque across the ankle complex while measuring motion at the ankle, subtalar, and ankle complex joints, by tracking motion of the tibia, talus, and calcaneus. A 6 degree-of-freedom tracker was pinned to each bone to measure 3D kinematics. A fourth tracker was used for system control and anatomical landmark digitization.

Passive motion was first tracked over the entire range of flexion/extension without the use of the torque sensor because of the large flexibility in this rotational direction. Subsequently, the torque sensor was used to manually apply and measure torque about the inversion/eversion and internal/external rotation axes of the AFT (Siegler et al., 1996). These torques were applied starting from three different joint positions within the full flexion arc: neutral (Neutral); maximum dorsiflexion (MaxDorsi), and maximum plantarflexion (MaxPlantar). The torques applied, measured and reported were those just required to reach the end of the range of motion in each condition. These tests were repeated for at least four loading-unloading cycles and replicated for the four joint conditions.

After testing the ankle in NATURAL, with the specimen still secured to the AFT, the surgeon used a standard surgical instrumentation for TAR (Giannini et al., 2010) to prepare the bone for the implantation, one at time, of each of the three implants. The tibiotalar articular surfaces were exposed by a standard anterior surgical approach. Bone preparation was performed by saws and drills with the support of the tibial jig. The CYL, TCM and SSCL implants were then tested. At the end, digitization of fiduciary markers for registration and of anatomical landmark for coordinate frame definitions (Cappozzo et al., 1995) was performed by using the ad-hoc optoelectronic tracker. For the latter, an established joint coordinate system convention (Grood and Suntay, 1983) was used to calculate dorsiflexion/plantarflexion (Dor-Pla), inversion/eversion (Inv-Eve) and internal/external rotation (Int-Ext), at the ankle, subtalar, and ankle complex joints.

For each specimen, each joint condition, each mechanical test and each repetition, collected data were first normalized to 0–100% of each passive or loading-unloading cycle. In order to isolate the effect of the artificial articular surfaces, differences between CYL, TCM and SSCL and the NATURAL conditions were calculated for each mechanical variable along the cycle. In addition, overall flexibility values were also obtained, here defined as the ratio between the total range of motion measured in the torque cycle and the corresponding maximum joint torque. These were tested for statistical significance as differences between intact and replaced joint conditions, using repeated-measure multifactor analysis of variance with a significance value of $p < 0.05$.

3. Results

Intra specimen repeatability, measured as the standard deviation of the repetitions, was smaller than 2.0 deg and 0.3 N m for joint rotation and flexibility, respectively (Belvedere et al., 2017).